# Measurement of the Ionospheric Reflection Height of an HF Wave in Vertical Incidence With a Resolution of Minutes

Leonardo A. Agüero Guzmán, Elias M. Ovalle, and Rodrigo A. Reeves, *Member, IEEE*

***Abstract*— In this letter, we present a prototype of an RF signal receiver operating in the HF band, whose design considers the use of software-defined radio signal processing technology, based on field-programmable gate arrays (FPGA) reconfigurable hardware and the use of gnuradio open software. The purpose of this letter is to improve the measurement rate at a fixed frequency of the reflection height, which is now obtained with a rate of 15 min using the IPS-42 ionosonde. The proposed method uses a pulse generated by the Canadian Advanced Digital Ionosonde as the transmitted signal. For the receiving section, the FPGA-based "Universal Software Radio Peripheral 1" was directly connected to a PC, where the return signals were analyzed by gnuradio. The measurements are taken with 1-min cadence, approximately, and are validated by comparing them with 15-min measurements taken with a colocated IPS-42 ionosonde. The acquisition rate of order 1 every minute is of interest in the study of a number of physical processes, i.e., traveling ionospheric disturbance, disturbances generated by seismic events, meteorological processes, and so on.**

***Index Terms*— Ionosonde, traveling ionospheric disturbances (TIDs), universal software radio peripheral (USRP).**

## I. Introduction

THE ionosphere is an ionized region over the surface of the Earth and exhibits an diurnal effect, as illustrated in Fig. 1, where it is shown a typical plasma density profile, as function of altitude. During the day, the main sources for ionization are electromagnetic radiation and high-energy particles being brought by the solar wind, but during the night, ionization by cosmic rays is the dominant factor [4], [5], [19].

The study of the ionosphere may be performed using instruments such as an ionosonde, coherent and incoherent radar wave scattering, GPS, and optical instruments. One of the most used instruments to study the ionosphere is the ionosonde that allows us to send a signal to the ionosphere where it gets reflected. These reflected echoes are received on the surface of the earth. The distance from the instrument to the place where the reflection occurs in the ionosphere is called virtual height, and can be calculated by measuring the time between the emission of the signal through the transmitter and the reception of the echo signal, considering that the electromagnetic wave propagates in vacuum, and therefore avoiding complicated assumptions on the chemical composition of the traveling path and its effects on the signal.

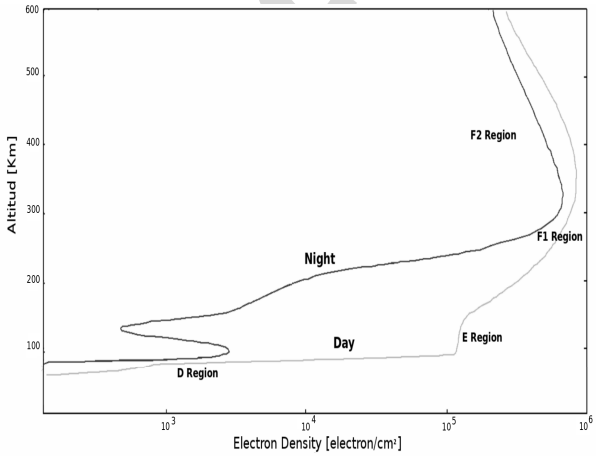


Fig. 1. Ionospheric electron density: typical plasma density profile, as function of altitude and also, it is shown the D, E, and F (F1 and F2) layers in the day (gray line) and the night (black line).

The knowledge and understanding of the ionosphere are currently relevant due to the strong relationship that exists with the new technologies, for example, with GPS satellites from which signals must transverse the ionosphere. Furthermore, it plays an important role in HF radio wave propagation because it allows the reflection of electromagnetic waves between 2 and 26 MHz in different layers. However, for a great solar activity, refracted signals can also be much higher than 26 MHz. The greater its density, the higher the frequencies that would be reflected. The production of free electrons and their distribution in the atmosphere are related to variations caused by various factors, including solar activity, seasons, sunspot cycle, traveling ionospheric disturbances (TIDs), earthquake, tsunamis, landslides or eruptions, meteorological processes, and so on. All these factors make ionospheric propagation to be variable over relatively short timescales. In Table I, we will discuss its effects and causes [3], [12], [15].

1) *TIDs*: These have been detected for several decades and by a number of different instruments, including ionosondes, incoherent scattering radars, and HF Doppler systems. These perturbations consist of a ripple or wave

Manuscript received October 7, 2017; revised February 3, 2018 and May 22, 2018; accepted June 14, 2018. The work of R. Reeves was supported in part by the Chilean Centro de Excelencia en Astrofísica y Tecnologías Afines (CATA) BASAL grant AFB-170002 and in part by Conicyt, Programa de Astronomía, Fondo Quimal 2018 Código 160012. *(Corresponding author: Leonardo A. Agüero Guzmán.)*

L. A. Agüero Guzmán is with the Departamento de Física, Universidad de Concepción, Casilla 160-C, Concepción, Chile (e-mail: leoaguero@udec.cl).

E. M. Ovalle is with the Departmento de Geofisica, Universidad de Concepción, Casilla 160-C, Concepcion, Chile.

R. A. Reeves is with CePIA, Departmento de Astronomía, Universidad de Concepción, Casilla 160-C, Concepcion, Chile.

Color versions of one or more of the figures in this letter are available online at http://ieeexplore.ieee.org.

Digital Object Identifier 10.1109/LGRS.2018.2856110

TABLE I
WAVES TYPES

| Type of disturbance | Ionospheric layer | Periods | Source |
|---|---|---|---|
| Planetary waves (PW) | F layer, summer | 2 - 5 days | Troposphere, The Mesosphere-Lower Thermosphere (MLT) |
| | F layer, Ecuatorial jet | 2 - 16 days | Troposphere, MLT |
| | F layer northern hemisfer | 2 - 30 days | Troposphere, MLT, variations by rotation (27-28 days) |
| Acoustic wave gravity (AWG) | Lower ionospheric | 10 - 180 min | Sun, meteorological and auroral activity, sunrise and sunset |
| | E, $E_s$ layer | $\geq$ 20 min | Sun, meteorological and auroral activity, sunrise and sunset |
| | F layer | 15 - 180 min | Auroral activity an energetic particles precipitations, thermosphere |
| TID | Large Scale (LSTID) | 0.5-3 hr | Disturbances in the high atmosphere and source before mentioned |
| | Medium Scale escala (MSTID) | 12 min-1 hr | Disturbances in the high atmosphere and source before mentioned |
| | Small Scale (SSTID) | 1-10 min | Disturbances in the high atmosphere and source before mentioned |
| Seismic events (Tsunamis) | E, F layers | 10 - 20 min | Submarine earthquake, landslides or eruptions |

in the electron density structure that propagates horizontally, causing the ions to be forced along the field lines by a pressure wave. There are three main types of TIDs [16]:

a) large-scale, with thousands of kilometers wavelengths;
b) medium-scale, with hundreds of kilometers wavelengths;
c) small scale, with tens of kilometers wavelengths.

2) *Planetary Waves*: Although its origin is tropospheric, these waves can be propagated by the ionosphere affecting global electrical currents. Their effects are mainly observed in the lower ionosphere and have oscillations with periods of 2–30 days and have been observed in all ionospheric layers [2].
3) *Gravity Waves*: It has an origin that is predominantly meteorological, although may be produced by earthquakes, volcanic eruptions, tornadoes, thunderstorms, solar eclipses, polar and equatorial electrojets, and so on. Their effects have been shown through both theoretical and experimental studies, identifying them as a mechanism for producing the transfer of energy and momentum from the troposphere to the ionosphere. These waves have periods between several minutes and a few hours [12], [15].
4) *Tsunamis and Earthquakes*: They refer to an impulsive movement of free surface (land or water), generating a vertical atmospheric pressure wave whose amplitude increases as the inverse of square root of density, which is required for the conservation of the wave kinetic energy [10], [11].
5) *Meteorological Process:* In the troposphere, there are many sources of strong internal waves that carry energy and momentum in the upward direction to the ionosphere. For example, climatological studies of gravity waves in the middle and upper atmosphere over Japan revealed almost continuous presence of gravity waves in the *F* region ([17], [18]).

For all these reasons, it is of great interest to obtain information on the ionospheric vertical structure, distribution, and variability in real time, at a rate higher than what is regularly obtained by conventional ionosondes. Currently, there are different alternatives that are not only more flexible and versatile but also offering low cost of implementation. The referred instrumentation is based on field-programmable gate arrays (FPGA) technology which are the hardware units that provide access to logic gates available to synthesize certain functionality. This enables significant signal processing in microwave systems to be implemented in digital form, and are configured and handled by software defined radio (SDR) technology, with a software-based interface to the hardware. In this letter, we accessed the hardware with an open source software called *Gnuradio*, which includes a well-developed graphical interface.


Fig. 2. USRP1.

### A. USRP Hardware

The Universal Software Radio Peripheral (USRP) (Fig. 2) board is our FPGA hardware interface of choice and the functionality is accessed with Gnuradio ([8], [9]). Basically, the USRP is an integrated board that incorporates analog to digital/digital to analog converters, some forms of RF frontend, and an FPGA that performs significant preprocessing of the input signal and can use daughter boards, such as RFX900, RFX1200, XCVR 2450, Basic TX/RX, and so on. These boards include filtering and heterodyne components for different frequency bands.

The USRP motherboard contains four 12-bit analog to digital converters (ADCs) and four 14-bit digital to analog converters (DACs) of high speed, with the sampling rate of 64 MS/s at the receiving and 128 MS/s at the transmitting stages, respectively. It also contains a programmable gain amplifier (PGA) before the ADCs that can amplify the input signal for the use of the entire bandwidth at the input of the ADCs. The full range of the ADCs is 2 V peak to peak, and the input is 50-$\Omega$ differential. The PGA is a software programmable card and can be used with a maximum gain of 20 dB.

In this letter, we use an improved USRP version, the Ettus USRP1, which provides entry-level RF processing capability. It is intended to enable the SDR development potential for cost-sensitive users and applications. The architecture includes an Altera Cyclone FPGA and universal serial bus 2.0

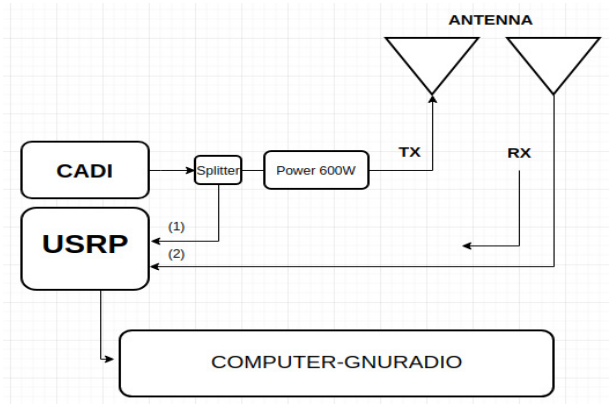


Fig. 3. Basic diagram for the system of transmission and reception.

TABLE II
CADI TRANSMISSION CHARACTERISTICS

| | | |
|---|---|---|
| Power output | 600W | 7.8kW (Baker 13) |
| Frequency range | 1-20MHz | |
| Frequency sweep time | 3s | |
| Pulse width | 40$\mu$s | 520$\mu$s (Baker 13) |
| Pulse interval | 25ms | |
| Height range | 90-1024km | |
| Configured frequency | 5.0MHz | |
| Range resolution | 6 km | |

connectivity to provide data to host processors. A modular design allows the USRP1 to operate from dc to 6 GHz. The USRP1 platform can support two complete RF daughter boards. This feature makes the USRP ideal for applications requiring high isolation between transmit and receive chains, or dual-band transmit/receive operation. The USRP1 can stream up to 8 MS/s to and from host applications, and users can implement custom functions in the FPGA fabric.

In our case, the USRP1 was interfaced with Basic TX/RX daughter boards, whose specifications are as follows:

1) *Basic Tx Daughter Board*: It is a low-cost daughter board that provides transmission capability from the USRP from 1 to 250 MHz. The BasicTx uses two wideband transformers to match the dual DAC outputs of a USRP to 50-Ω SubMiniature version A connections.
2) *Basic Rx Daughter Board*: It is a low-cost daughter board that provides direct access to the ADC inputs. The board can accept real-mode signals from 1 to 250 MHz.

The Basic RX/Basic TX is ideal for applications using an external front end providing relatively clean signals within the operational bandwidth. Wideband transformers couple each RF input to a single channel of the USRP's ADC. The signals sampled by the ADC are manipulated in the FPGA and can be processed as two real-mode signals, or a single I-Q pair. Given that the frequency range of our application is right within the bandwidth of the daughter boards, we do not need to include in our setup the extra front-end components.

## II. EXPERIMENTAL SETUP

For this letter, we combined the Canadian Advanced Digital Ionosonde (CADI) (Digital Ionosonde [6], [7]) capabilities

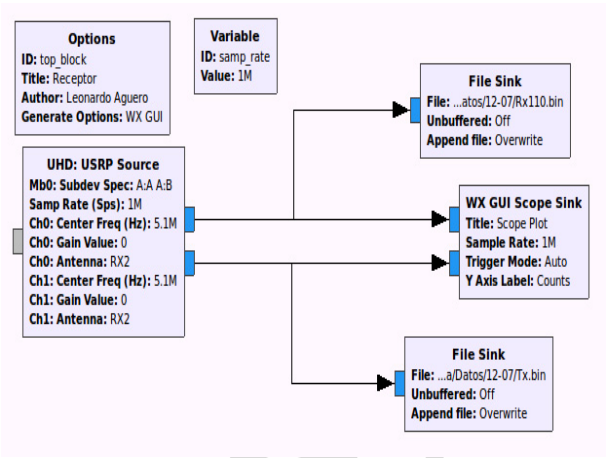


Fig. 4. Dual-channel receiver system.

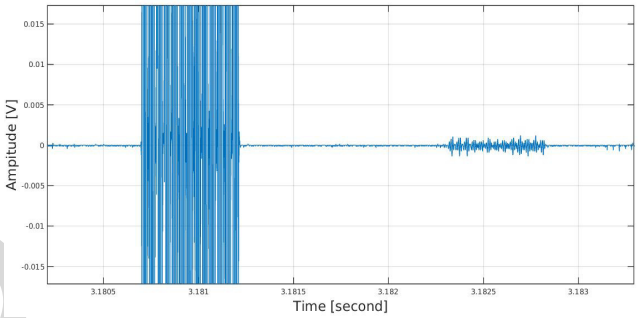


Fig. 5. Transmitted and received pulse on USRP and visualized by a MATLAB script.

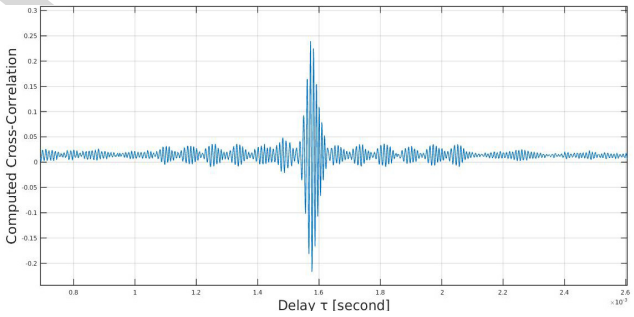


Fig. 6. Visual cross correlation results between the transmitted and received pulses on USRP.

for the transmission of an RF pulse to the ionosphere with the digital receiver capabilities of the USRP1. The hardware was configured and operated by gnuradio. Consequently, the time travel for the transmitted pulse to get reflected in the ionospheric reflective screen and return to the receiver gives an estimate of the height at which the reflective layer locates in the ionosphere, which is called the virtual height because it assumes that vacuum is the transmission media. Currently, the conventional ionosonde we operate at our facilities (see the following), sends a pulse train to the ionosphere with frequencies ranging between 1 and 25 MHz and every 15 min, generating an ionogram, which allows studying the variability in the height of the ionosphere with periodicities of about an hour.

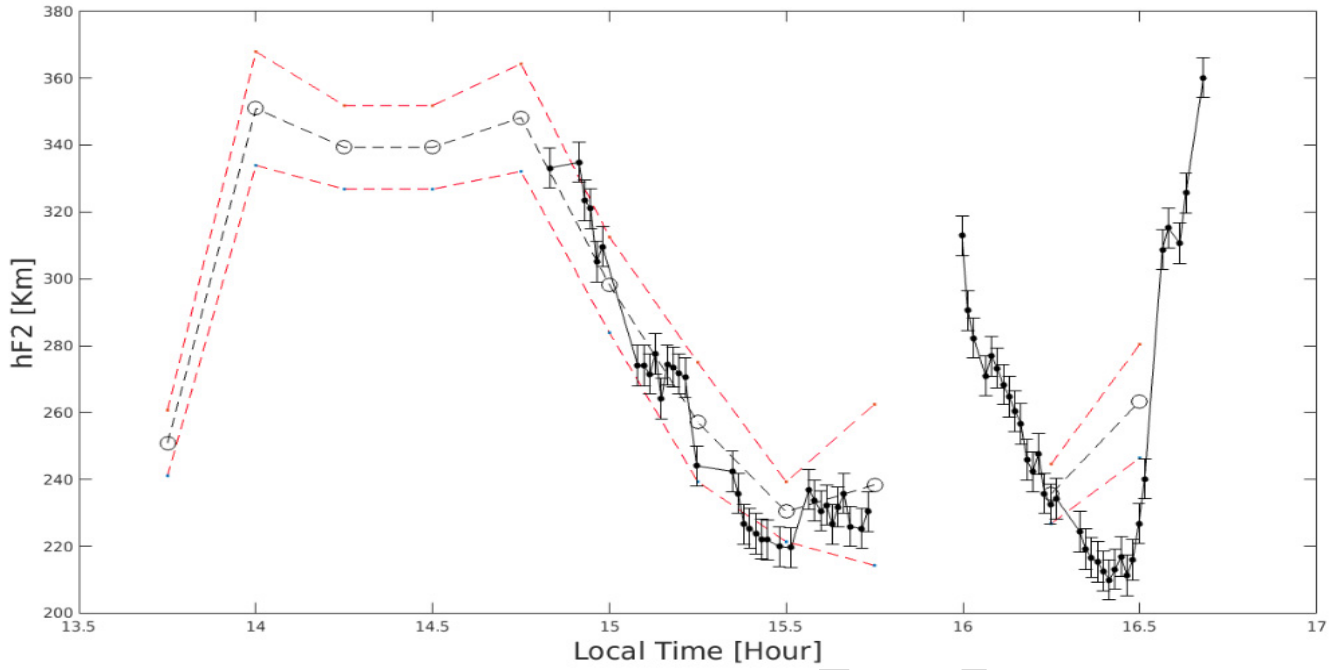


Fig. 7. Empty circles: measurements made with the IPS-42 ionosonde each 15 min. Dotted lines: band for measurement errors. Black full circles: measurements made using our USRP system. Error bars: range-resolution of the radar equation 3.

Given the high recurrence of seismic phenomena in certain parts of the world, and particularly in Chile where our facilities are located, we are interested in the study of ionospheric disturbances caused by the propagation of gravity waves generated either by earthquakes or tsunamis, which have a variability on the order of minutes. As these measurements cannot be made with our conventional ionosondes, we decided to develop a system that would allow us to obtain the variation of the virtual height at a fixed frequency and with 1-min cadence, using the ionosonde as a transmitter, and receive the reflected pulses with the digital receiver.

Fig. 3 illustrates a diagram of our system for the combined architecture of a CADI ionosonde as transmitter, and receiving the signal using a dual-channel receiver based on USRP1/ Gnuradio. The signal generated by CADI is divided into two equal signals (splitter), one feeds to the 600-W transmitter and the other passes through a 2-dB attenuator to the channel 1. In the reception, the signal reflected in the ionosphere is measured by the USRP into the channel 2. Table II illustrates the CADI technical characteristics as a transmitter.

For correct operation of the instrument, we need to configure two signals. The first signal is sent to the reflecting layer by the CADI transmitter, and the second signal being measured by the USRP. These two signals, tuned at 5 MHz, feed the USRP on channels 0 and 1 and are transformed to IF frequency (100 KHz) with two common local oscillators tuned at 5.1 MHz. The ADCs are configured with a sample rate of 1 MS/s (superior to the Nyquist frequency of 200 KS/s). As shown in Fig. 4, the flow graph consists of several blocks.

## III. Experiment and Data Analysis

In our experiment, the CADI ionosonde is an existing equipment of the new ionospheric station (j3p) in Chile, located in Chillán (36° 38′ 29″S; 71° 59′ 41″W) at Universidad Adventista de Chile [1]. The frequency used in pulse transmission was 5.0 MHz due to two factors: 1) ionograms obtained by the IPS-42 show that the ionospheric layers are best constituted between 2 and 6 MHz. From this analysis, we conclude that this frequency range should be used to attempt such experiment, and 2) because, at that frequency, the Tx/Rx antennas showed a dip in return loss measured with vector network analyzer, and also the ionograms observed from the ionosonde IPS-42 showed a good and stable behavior of the ionospheric profiles at that particular frequency.

The measurements were taken on July 12, 2017. The disturbance storm time values ranged from $-13$ to $-5$, and the observed F10.7 solar radio flux was 77.58, i.e., measurements were made in quiet solar and geomagnetic conditions. Fig. 5 shows the pulse transmitted by CADI with an amplitude $80\times$ bigger than the received pulse by the USRP, with a difference in time (delay) of 1.577 ms, which corresponds to a reflection height of 240 km on average. Fig. 6 shows the cross correlation between both pulses and it allows us to estimate the travel time to the reflective layer in the ionosphere.

### A. Cross Correlation

In signal processing, cross correlation is a measure that allows us to evaluate the similarity between the two signals as a function of the displacement of one relative to the other, as a function of the time lag between them.

We first consider the cross correlation function of two signals, $x(t)$ and $y(t)$, of a real variable

$$r_{xy}(\tau) = \int_{-\infty}^{\infty} x(t) \cdot y(t-\tau) d\tau \quad (1)$$

where $\tau$ is the displacement, also known as the lag.

By properties of the cross correlation function, if $x(t) = a \cdot y(t-T)$, where **'a'** is a numeric factor, i.e., $x(t)$ is a scaled and delayed version of $y(t)$, then $r_{xy}$ will have its maximum value at $\tau = T$.

In ideal conditions, if $x(t)$ is the signal transmitted and $y(t-T)$ is signal reflected by an object at a distance $R$ and received in a time $T$ (delay), then the range ($R$) or distance target is calculated using

$$R = \frac{c \cdot T}{2} \tag{2}$$

where $c$ is the speed of light.

Now, each $R$ range has an associated resolution in height that is related to bandwidth of the transmitted pulse ($B_{\mathrm{TX}}$). In a pulse compression system, such as CADI, the range resolution of the radar is given by the length of the pulse II; in our case, $B_{\mathrm{TX}} = 25$ KHz

$$\Delta R = \frac{c}{2 \cdot B_{\mathrm{TX}}}. \tag{3}$$

The observed time delay between the transmitted and the received signals was estimated using a cross correlation implementation in MATLAB. To validate our measurements, reflection height comparisons were concurrently taken with an IPS-42 ionosonde working at the same site, which was operated every 15 min. Fig. 7 shows the simultaneous reflection heights for an F2 ionosphere layer, measured by a typical ionosonde as IPS-42, every 15 min (circles connected by dotted lines) and by the developed system presented in this letter (black full circles connected with error bars given by 3, which provides the uncertainty in the derived virtual height, with a rate of one measurement per minute. The figure shows the validate of our measurement.

## IV. Conclusion

This letter introduces the design and implementation of a hybrid radar system of scientific importance for the HF-band. This instrument considers the use of SDR signal processing technology, (*gnuradio* free code) and a USRP1 unit. The system allowed us to improve the measurement rate at a fixed frequency from 15 min (using IPS-42 ionosonde) to 1 min. The reliability of the design was verified through several experiments in the laboratory and validated with 15-min measurements taken with IPS-42 ionosonde. The new radar structure design combines a pulse generated by a CADI ionosonde, and a USRP1 commanded by gnuradio connected to a PC, where the signal is recorded. The data are analyzed offline using cross correlation analysis programmed in MATLAB.

The development of the presented system represents the progress in the study of ionospheric dynamics in our country, and contributes to the understanding of its physical processes associated with minute temporal variations for 5-MHz wave reflected in the ionosphere. We hope that in the near future, the proposed system could be used to detect TIDs and disturbances generated by a seismic activity.

## Acknowledgment

The authors would like to thank the CePIA laboratory at the Astronomy Department and Telecommunications in the Electrical Engineering Department at Universidad de Concepcion, for instrumental support. They would also like to thank the j3p Ionospheric Observatory for their ionosondes and for making the facilities available.

## References

[1] L. A. A. Guzmán, "Instalación de una estación ionosferica y su puesta en marcha," M.S. thesis, Dept. Phys., Univ. Concepción, Concepción, Chile, 2014.

[2] L. F. Alberca, D. Altadill, J. Solé, E. Galdón, and E. M. Apostolov, "Contribución del observatorio del Ebro al estudio de la ionosfera terrestre," *Fisica Tierra*, vol. 12, pp. 13–39, 2000.

[3] J. Artru, V. Ducic, H. Kanamori, P. Lognonne, and M. Murakami, "Ionospheric detection of gravity waves induced by tsunamis," *Geophys. J. Int.*, vol. 160, no. 3, pp. 840–848, 2005.

[4] *Introduction to HF Radio Propagation*, Austral. Government–IPS Radio Space Services, Australia, 2016.

[5] G. Breit and M. A. Tuve, "A test of the existence of the conducting layer," *Phys. Rev.*, vol. 28, no. 3, pp. 554–557, 1926.

[6] *CADI*. Accessed: 2017. [Online]. Available: http://www.sil.sk.ca/content/cadi

[7] *The Canadian Advanced Digital Ionosonde: Design and Results*. Accessed: 2017. [Online]. Available: http://www.sws.bom.gov.au/IPSHosted/INAG/uag-104/text/macdoug.html

[8] *USRP1*. Accessed: 2017. [Online]. Available: https://www.ettus.com/product/details/USRPPKG

[9] *Universal Software Radio Peripheral*. Accessed: 2017. [Online]. Available: https://en.wikipedia.org/wiki/Universal_Software_Radio_Peripheral

[10] C. O. Hines, "Internal atmospheric gravity waves at ionospheric heights," *Can. J. Phys.*, vol. 38, pp. 1441–1481, Nov. 1960.

[11] C. O. Hines, "Gravity waves in the atmosphere," *Nature*, vol. 239, pp. 73–78, Sep. 1972.

[12] K. Hocke and K. Schlegel, "A review of atmospheric gravity waves and travelling ionospheric disturbances: 1982–1995," *Ann. Geophys.*, vol. 14, no. 9, pp. 917–940, 1996.

[13] *Nomenclature of the Frequency and Wavelength Bands Used in Telecommunications*, document, ITU-R, 2015, Art. no. E 70000.

[14] A. S. Jursa, *Handbook of Geophysics and the Space Environment*, vol. 1. Washington, DC, USA: Air Force Interim Report, 1985.

[15] J. Lastovicka, "Forcing of the ionosphere by waves from below," *J. Atmos. Sol.-Terr. Phys.*, vol. 68, pp. 479–497, Feb. 2006.

[16] R. Leitinger and M. Rieger, "The TID model for modulation of large scale electron density models," *Ann. Geophy.*, vol. 48, no. 3, pp. 515–523, 2005.

[17] W. L. Oliver, Y. Otsuka, M. Sato, T. Takami, and S. Fukao, "A climatology of F region gravity wave propagation over the middle and upper atmosphere radar," *J. Geophys. Res., Space Phys.*, vol. 102, no. A7, pp. 14499–14512, 1997.

[18] T. Šindelárová, D. Buresova, and J. Chum, "Observations of acoustic-gravity waves in the ionosphere generated by severe tropospheric weather," *Stud. Geophys. Geodaetica*, vol. 53, pp. 403–418, Jul. 2009.

[19] J. Ratcliffe, *Sun, Earth, and Radio: An Introduction to the Ionosphere and Magnetosphere*. London, U.K.: Weidenfeld & Nicholson, 1970.